© 2020. Published by The Company of Biologists Ltd | Development (2020) 147, dev187047. doi:10.1242/dev.187047

RESEARCH REPORT

Mitf-family transcription factor function is required within cranial neural crest cells to promote choroid fissure closure

Katie L. Sinagoga[1], Alessandra M. Larimer-Picciani[1], Stephanie M. George[1], Samantha A. Spencer[2], James A. Lister[2] and Jeffrey M. Gross[1,*]

ABSTRACT

A crucial step in eye development is the closure of the choroid fissure (CF), a transient structure in the ventral optic cup through which vasculature enters the eye and ganglion cell axons exit. Although many factors have been identified that function during CF closure, the molecular and cellular mechanisms mediating this process remain poorly understood. Failure of CF closure results in colobomas. Recently, *MITF* was shown to be mutated in a subset of individuals with colobomas, but how MITF functions during CF closure is unknown. To address this issue, zebrafish with mutations in *mitfa* and *tfec*, two members of the Mitf family of transcription factors, were analyzed and their functions during CF closure determined. *mitfa;tfec* mutants possess severe colobomas and our data demonstrate that Mitf activity is required within cranial neural crest cells (cNCCs) during CF closure. In the absence of Mitf function, cNCC migration and localization in the optic cup are perturbed. These data shed light on the cellular mechanisms underlying colobomas in individuals with *MITF* mutations and identify a novel role for Mitf function in cNCCs during CF closure.

KEY WORDS: Coloboma, Choroid fissure, Mitf, Neural crest, Zebrafish

INTRODUCTION

The development of the vertebrate eye is a complex process, involving coordinated morphogenesis, migration and communication between the surface ectoderm, neural ectoderm and extraocular mesenchyme. During eye development, the optic primordia evaginate from the ventral forebrain and give rise to the optic vesicles (Bibliowicz et al., 2011). Subsequent invagination of the vesicle gives rise to the optic cup, which eventually subdivides into the neural retina and retinal pigmented epithelium (RPE). During optic cup morphogenesis the optic stalk narrows ventrally and creates a transient opening, known as the choroid fissure (CF) (FitzPatrick, 2005). The CF is crucial for the entrance of the hyaloid vasculature into the eye and the exit of retinal ganglion cell axons. The CF must eventually close, such that retinal and RPE tissues are contained within the optic cup.

The CF is a remarkable area within the eye, in that it is the point of convergence for the retina, RPE and subtypes of periocular mesenchyme (POM). A network of intrinsic factors and signaling and regulatory pathways influences CF closure (ALSomiry et al., 2019). The intersection of these major pathways mediates the transcription of downstream target genes within the CF but also in the surrounding POM, which subsequently influences optic cup morphogenesis. The POM plays a crucial role in this process, as mesenchymal cells physically interact with and signal to the CF and optic cup to facilitate optic cup morphogenesis and CF closure (Bryan et al., 2020; Fuhrmann et al., 2000; Gestri et al., 2018; James et al., 2016). A large proportion of POM cells are derived from cranial neural crest cells (cNCCs) (Williams and Bohnsack, 2015). Neural crest cells (NCCs) are born from the dorsal neural tube, after which they migrate ventrally and differentiate into mesenchymal components of the face (Bohnsack et al., 2011; Christiansen et al., 2000; Kaucka et al., 2016; Williams and Bohnsack, 2015). cNCCs additionally migrate anteriorly around the optic vesicle, during which they communicate with the optic stalk and retina (Grocott et al., 2011). Ultimately, morphogenetic and signaling events between the RPE, retina and cNCC-derived-POM facilitate the breakdown of basement membrane components within the fissure (Bryan et al., 2020; James et al., 2016; Lee and Gross, 2007), which enables fusion between the retina and RPE components of the CF. Despite these studies, the cellular and molecular underpinnings of CF closure remain unclear, with ECM interactions, signaling pathways and a variety of transcription factors implicated in the process. Confounding this further, closure involves three distinct cell types: retina, RPE and POM.

When CF closure is perturbed, colobomas result. Colobomas are estimated to occur in 1 in 10,000 live births and severe cases account for up to 10% of childhood blindness (Bermejo and Martínez-Frías, 1998; Onwochei et al., 2000; Stoll et al., 1997). Depending on where along the proximal-distal axis of the CF closure fails, one or several parts of the eye can be involved (Gregory-Evans et al., 2004). Although causative mutations have been identified in some coloboma patients, these loci only account for ∼20% of reported cases (Chang et al., 2006; FitzPatrick, 2005). Recently, mutations were identified in *MITF*, a member of the microphthalmia-associated transcription factor/TFE family of transcription factors (TFs), that result in colobomas (George et al., 2016). Individuals with compound heterozygous mutations in *MITF* display a phenotype termed COMMAD syndrome (coloboma, osteoporosis, microphthalmia, macrocephaly, albinism and deafness). MITF TFs are well known for their roles in pigmentation, melanocyte development and RPE specification (Bharti et al., 2012; Hsiao and Fisher, 2014; Lister, 1999; Martina et al., 2014). *MITF* mutations are also associated with melanomas and with diseases like Waardenburg syndrome type IIA, which presents with pigmentary abnormalities and congenital sensorineural hearing loss (Kawakami and Fisher, 2017). Dominant-negative mouse Mitf mutations ($Mitf^{mi/mi}$) result in colobomatous microphthalmia (Hero, 1989;

[1]Departments of Ophthalmology and Developmental Biology, Louis J. Fox Center for Vision Restoration, The University of Pittsburgh School of Medicine, Pittsburgh, PA 15213, USA. [2]Department of Human and Molecular Genetics, Virginia Commonwealth University School of Medicine, Richmond, VA 23298, USA.

*Author for correspondence (grossjm@pitt.edu)

J.M.G., 0000-0002-9422-6312

Handling Editor: John Wallingford
Received 8 December 2019; Accepted 29 May 2020

Development (2020) 147, dev187047. doi:10.1242/dev.187047

Takebayashi et al., 1996), and loss of MITF in human embryonic stem cells impairs proliferation in optic vesicles differentiated from these cells (Capowski et al., 2014), which also highlights the crucial role of MITF in the gene regulatory network regulating retina/RPE development. *MITF* mutations in COMMAD patients result in decreased MITF nuclear localization and DNA-binding ability (George et al., 2016). However, despite these biochemical results, little is known about how MITF contributes to CF closure.

The Mitf family of TFs includes four members: MITF, TFEC, TFEB and TFE3 (Martina et al., 2014; Steingrímsson et al., 2004; Zhao et al., 1993). MITF TFs homodimerize or heterodimerize with one another and bind to E-box and M-box DNA regions to regulate transcription of downstream targets (Hemesath et al., 1994; Pogenberg et al., 2012). MITF is the most well-studied member of the family, with functions identified in cell cycle regulation, motility, metabolism, cell survival and pigmentation (Cavodeassi and Bovolenta, 2014; Hsiao and Fisher, 2014). In addition to paralogous genes in zebrafish (*mitfa* and *mitfb*), there are at least nine isoforms of Mitf/MITF, each maintaining a specific expression pattern in developing mouse and zebrafish embryos (Bharti et al., 2008; Lister et al., 2001). Many mitf isoforms have overlapping expression in zebrafish, but *mitfa* is expressed specifically in cNCCs, neural crest-derived melanocytes and the developing RPE (Lister et al., 2001). *tfec* has a similar expression pattern to *mitfa* in the zebrafish eye (Lister et al., 2011). Although expressed in the RPE and cNCCs during early eye development, *tfec* is also upregulated in the CF during closure (Cao et al., 2018). Owing to the convergence of RPE and cNCC-derived POM in the CF, it remains unknown in which cell type(s) mitf TFs function to promote closure.

Ocular development and morphogenesis are highly conserved between zebrafish and humans, making this an ideal system with which to study CF closure. Using a novel *mitfa;tfec* mutant line, we demonstrate that the loss of these Mitf-family TFs phenocopies colobomas observed in *MITF* individuals. Both RPE and cNCC development are perturbed in *mitfa;tfec* mutants. Through a series of embryological manipulations and rescue experiments, we demonstrate that Mitf-family function is required within the cNCCs to facilitate CF closure. Furthermore, our data suggest that Mitf TFs act within cNCCs to promote their localization in/around the eye and their survival. These data identify potential cellular underpinnings of colobomas in human COMMAD patients with mutations in *MITF*, and provide a platform through which cNCC-specific functions during CF closure can be further elucidated.

RESULTS AND DISCUSSION

Previous studies have shown that $mitfa^{-/-}$ mutants possess pigmentation defects but have normal ocular development (Lister, 1999). Mitf-family members are co-expressed in many tissues and, in zebrafish, *mitfa* and *tfec* have similar expression patterns within the RPE and cNCCs (Lister et al., 2001, 2011). Therefore, using CRISPR/Cas9, we generated a *tfec* mutant (Fig. S1). $tfec^{vc60}$ contains a frameshifting indel in exon 7, which encodes the second helix of the dimerization domain, resulting in a complete loss of function (Petratou et al., 2019 preprint). $tfec^{-/-}$ mutants did not live beyond larval stages as their swim bladders failed to inflate. $tfec^{-/-}$ mutants also possessed pigmentation defects and were mildly microphthalmic, but optic cup formation was normal and they displayed no obvious signs of colobomas (Fig. S1).

Considering that there may be developmental compensation and/or functional redundancy between these genes, we next generated $mitfa^{-/-};tfec^{-/-}$ mutants and assessed eye development. At 4 days postfertilization (dpf), $mitfa^{-/-};tfec^{-/-}$ mutants displayed prominent bilateral colobomas (Fig. 1A). Only $mitfa^{-/-};tfec^{-/-}$ mutants possessed colobomas; CF closure was normal in $mitfa^{-/-};tfec^{+/+}$ (Fig. 1A) and $mitfa^{-/-};tfec^{+/-}$ embryos. $mitfa^{-/-};tfec^{+/-}$ mutants were viable and therefore for the remainder of the experiments, $mitfa^{-/-};tfec^{+/-}$ incrosses were used to generate $mitfa^{-/-};tfec^{-/-}$ mutants. Through this breeding scheme, expected Mendelian ratios of mutant embryos were recovered and colobomas appeared, on average, in 21% of progeny (Fig. S2). Colobomas vary in their severity in most models of the disease, as well as in human patients, and we likewise observed a range of severities in $mitfa^{-/-};tfec^{-/-}$ mutants, as assessed by the angle of CF opening (Fig. 1B).

CF closure is a multistep process that relies on the breakdown of the basement membrane (BM) lining the tightly apposed sides of the CF (Bernstein et al., 2018; Carrara et al., 2019; James et al., 2016). A hallmark of colobomas in many models of the disease is BM retention within the CF (Barbieri et al., 2002; Geeraets, 1976; Hero, 1990; Hero et al., 1991; James et al., 2016; See and Clagett-Dame, 2009; Tsuji et al., 2012). Using laminin as a marker of the BM, we assayed BM degradation in $mitfa^{-/-};tfec^{-/-}$ mutants. $mitfa^{-/-};tfec^{-/-}$ mutants retained strong laminin expression in the CF, whereas $mitfa^{-/-};tfec^{+/+}$ controls have degraded the intervening BM by 48 h postfertilization (hpf) (Fig. 1C).

mitfa and *tfec* are expressed in two distinct cellular populations within the developing eye: the RPE and cNCCs (Lister et al., 1999, 2011). Activity in one or both of these tissues could mediate CF closure events that are disrupted in COMMAD patients. With this in mind, we examined the development of these two cell types in $mitfa^{-/-};tfec^{-/-}$ mutants. At 48 hpf, there was a dose-dependent effect on RPE pigmentation: the RPE of 'control' $mitfa^{-/-};tfec^{+/+}$ embryos was normally pigmented, whereas it was hypopigmented in $mitfa^{-/-};tfec^{+/-}$ mutants; and $mitfa^{-/-};tfec^{-/-}$ mutants were barely pigmented (Fig. 2A). However, these RPE pigmentation differences resolved by 4 dpf. To examine cNCC development in $mitfa^{-/-};tfec^{-/-}$ mutants, we used a *mitfa*:GFP transgene that labels a subset of migratory cNCCs but not RPE (Curran et al., 2009). At 24 hpf, control embryos had 0.6813±0.051 cNCCs per 1000 µm^2 of optic cup, whereas mutants displayed 0.3658±0.029 cNCCs per 1000 µm^2 (P=0.0007, Fig. 2B). Notably, when we examined sections beyond the anterior/ocular region, *mitfa*:GFP$^+$ cNCCs were consistently detected near the neural tube rather than approaching the eye (Fig. 2B). Transverse serial sections taken from $mitfa^{-/-};tfec^{+/+}$;*mitfa*:GFP (control) and $mitfa^{-/-};tfec^{-/-}$;*mitfa*:GFP mutants showed substantially fewer cNCCs within the POM of $mitfa^{-/-};tfec^{-/-}$ mutants at 48 hpf (Fig. 2C). To address the possibility of developmental delay, whole-mount imaging of $mitfa^{-/-};tfec^{+/-}$;*mitfa*:GFP and $mitfa^{-/-};tfec^{-/-}$;*mitfa*:GFP mutants was performed at 48 hpf and 72 hpf (Fig. S3A). Mutant embryos also lacked cNCCs surrounding the optic cup, suggesting that $mitfa^{-/-};tfec^{-/-}$ mutants do not regain the *mitfa*:GFP cNCC contribution to the POM at later developmental stages.

Optic cup invagination and CF formation occurs from 16 hpf to 24 hpf (Schmitt and Dowling, 1994). At the same time, cNCCs are being specified from the dorsal neural tube and will migrate anteriorly around the eye (Christiansen et al., 2000), with the eye thought to provide a source of attractant for their migration (Langenberg et al., 2008). Given the decrease in cNCCs in the POM of $mitfa^{-/-};tfec^{-/-}$ mutants, we predicted that the localization of cNCCs in the eye field was perturbed. Using *in vivo* 4D time-lapse imaging, we followed the migration of *mitfa*:GFP$^+$ cNCCs for 15 h starting at 25 hpf (Movies 1 and 2). $mitfa^{-/-};tfec^{-/-}$ cNCCs did not migrate from the dorsal neural tube to the eye. From the time-

Development (2020) 147, dev187047. doi:10.1242/dev.187047

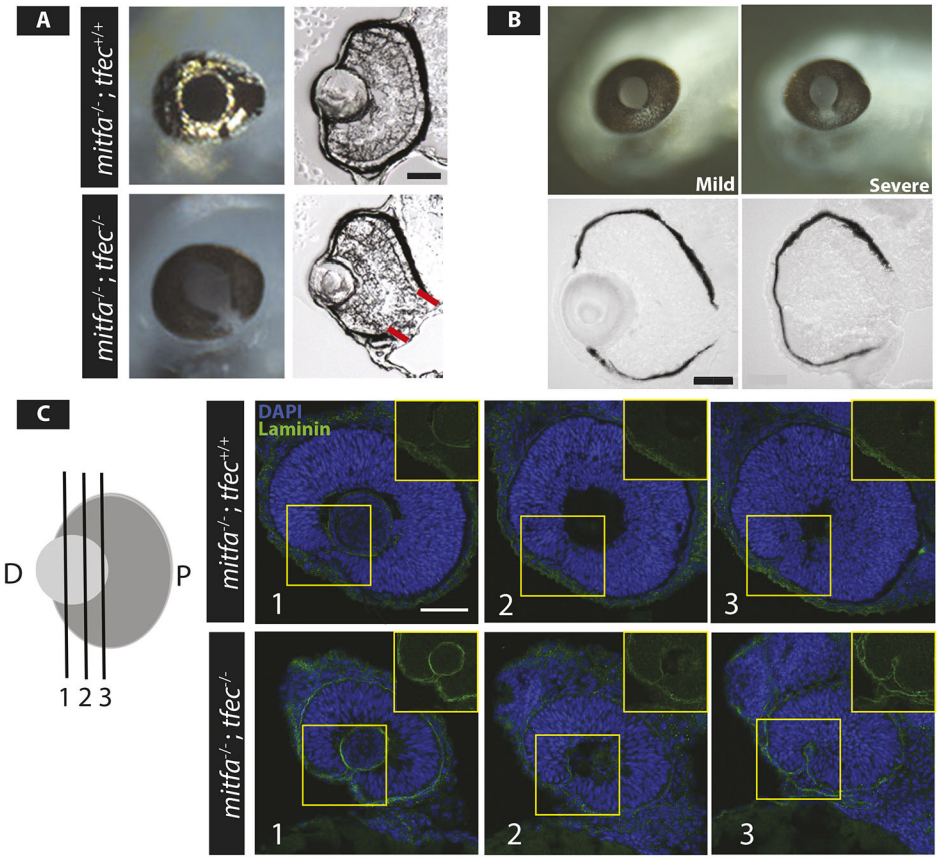

Fig. 1. Zebrafish *mitfa;tfec* mutants phenocopy human colobomas. (A) At 4 dpf, *mitfa*$^{-/-}$;*tfec*$^{-/-}$ mutants possess colobomas (outlined in red), with a range of severity (B). (C) At 48 hpf, serial sections through the distal (D) to proximal (P) axis of the CF reveal persistent expression of laminin in the *mitfa*$^{-/-}$;*tfec*$^{-/-}$ mutant CF. The boxes indicate the areas enlarged in the insets showing laminin staining within the CF. Dorsal is upwards in all images. Scale bars: 50 µm.

lapse data, some cNCCs in *mitfa*$^{-/-}$;*tfec*$^{-/-}$ mutants appeared to burst (see t=8:08-10:08 in Movie 2), consistent with cell death during their migration. To directly assess whether elevated apoptosis contributed to the lack of cNCCs around the eye of *mitfa*$^{-/-}$;*tfec*$^{-/-}$ mutants, we performed TUNEL staining at 24 hpf. Although the number of TUNEL^{+} cNCCs was elevated in *mitfa*$^{-/-}$;*tfec*$^{-/-}$ mutants, the difference was not significant when compared with wild-type controls, suggesting that lack of cNCCs within the POM could be driven by a defect in cell migration (Fig. S3B). Combined, these data demonstrate a transient delay in RPE pigmentation in the absence of mitfa/tfec function and a significant defect in cNCC localization to the POM in *mitfa*$^{-/-}$;*tfec*$^{-/-}$ mutants.

Ocular hypopigmentation or albinism is a common feature of a number of human disorders but they do not commonly correlate with colobomas, and most defects in RPE formation/function do not result in colobomas (e.g. Ma et al., 2019; Fuhrmann 2010; Reissmann and Ludwig, 2013; Jeffery 1998). On the other hand, there are many studies demonstrating functional requirements for cNCCs and POM in regulating early eye development and CF closure (Akula et al., 2019; Bryan et al., 2020; Dee et al., 2013; Fuhrmann et al., 2000; Gestri et al., 2018; James et al., 2016; Lupo et al., 2011; McMahon et al., 2009; Sedykh et al., 2017). Although our imaging data demonstrate abnormalities in the cNCC population of *mitfa*$^{-/-}$;*tfec*$^{-/-}$ mutants, given that Mitf-family genes are expressed in both RPE and cNCCs, it remains possible that defects within the RPE could also contribute to colobomas. Thus, we wanted to determine in which cell population *mitfa* and *tfec* function was required to close the CF. Zebrafish are highly amenable to embryonic transplantation experiments, in which cells can be transplanted between embryos to create genetic mosaics (Carmany-Rampey and Moens, 2006), with cells targeted to specific tissues or cell types based on established fate maps (Woo and Fraser, 1995) to determine in which cell type(s) a gene product functions.

To test the hypothesis that Mitf-family function was required in cNCCs during CF closure, we transplanted wild-type cells into the cNCC domain (Fig. 3A) or the retina/RPE domain (Fig. 3C) of *mitfa*$^{-/-}$;*tfec*$^{-/-}$ mutant host embryos, and quantified CF closure at 4 dpf. Donor embryos were injected with fluorescein isothiocyanate-dextran at the one- or two-cell stage to track their progeny in hosts and validate correct targeting. Wild-type cells transplanted into the cNCC-fated domain in *mitfa*$^{-/-}$;*tfec*$^{-/-}$ mutants resulted in a population of strongly labeled cNCCs at 24 hpf (Fig. 3A). Remarkably, wild-type cNCCs rescued CF closure in *mitfa*$^{-/-}$;*tfec*$^{-/-}$ mutants (Fig. 3B, Fig. S4C). Qualitatively, the CF appeared fully closed in six out of seven transplanted mutants when examined in whole mount (Fig. 3B). Quantitatively, the maximum angle of CF opening in serial sections from non-transplanted mutant eyes was 26.9°±3.04°, whereas in *mitfa*$^{-/-}$;*tfec*$^{-/-}$ mutants containing wild-type cNCCs, it was reduced to 10.33°±2.65° (P=0.0004; Fig. 3E). Transplantation of wild-type cells into the cNCC domain of *mitfa*$^{-/-}$;*tfec*$^{+/-}$ embryos had no effect (Fig. S4A). These data indicate that Mitf-family function in cNCCs is sufficient to mediate CF closure in *mitfa*$^{-/-}$;*tfec*$^{-/-}$ mutants. Wild-type cNCCs also retained the ability to migrate to the eye of *mitfa*$^{-/-}$;*tfec*$^{-/-}$ mutants (Fig. 3B), supporting a cell-autonomous role for *mitfa* and *tfec* within cNCCs in mediating their migration to the eye.

We next tested the alternative hypothesis, that Mitf-family function was required in the retina/RPE to enable CF closure. Wild-type cells transplanted into the retina/RPE-fated domain of *mitfa*$^{-/-}$;*tfec*$^{-/-}$ mutants resulted in a strongly labeled optic cup at 24 hpf (Fig. 3C). Only embryos in which at least 20% of the optic cup was

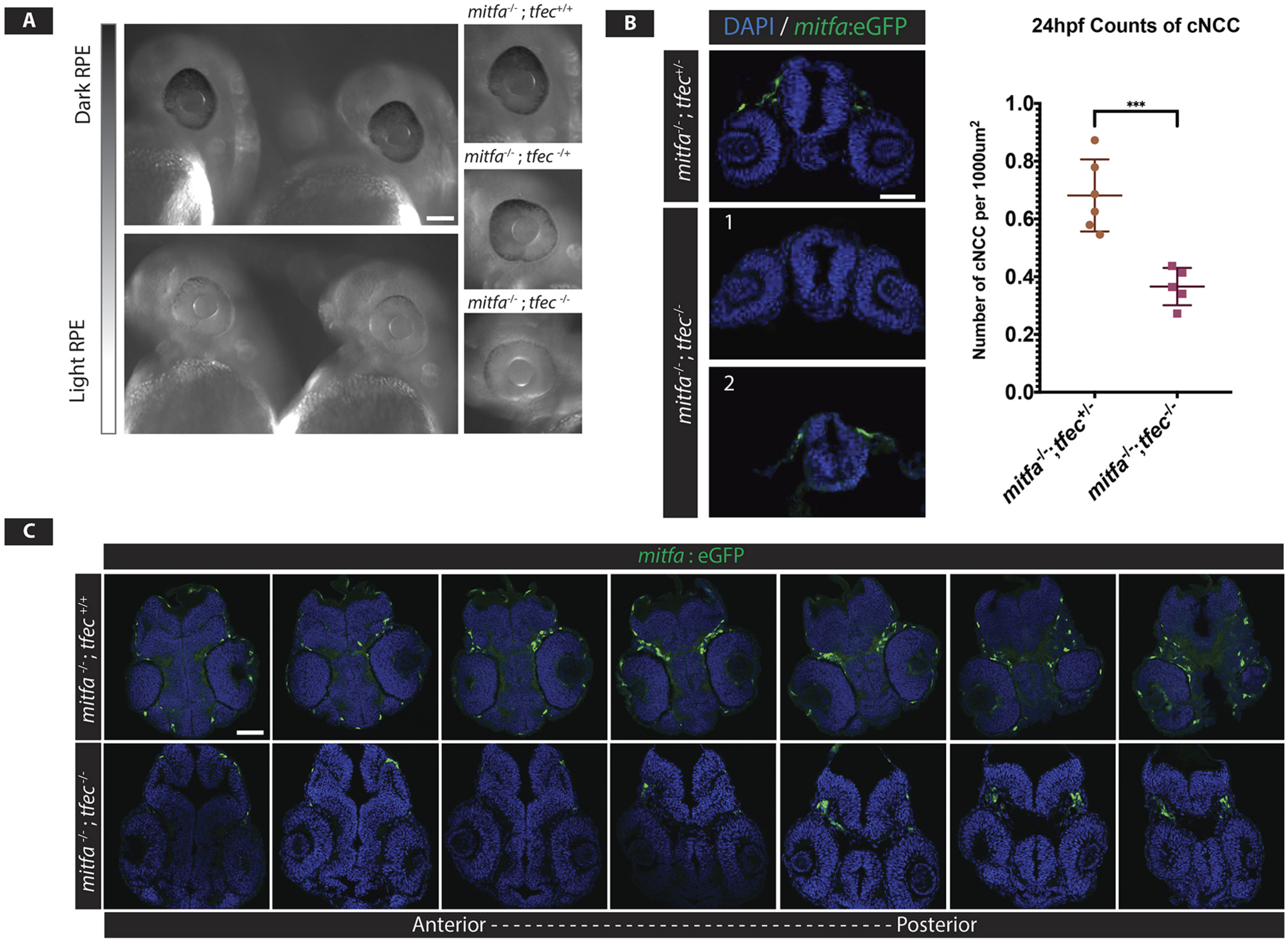

Fig. 2. *mitfa*$^{-/-}$*;tfec*$^{-/-}$ mutants display RPE and cNCC phenotypes. (A) At 48 hpf, *mitf*$^{-/-}$*;tfec*$^{+-/-}$ and *mitfa*$^{-/-}$*;tfec*$^{-/-}$ mutants display mild to severe hypopigmentation, respectively. The RPE eventually becomes normally pigmented by 4 dpf in both genotypes. (B) At 24 hpf, fewer cNCCs are present around the eye of *mitfa*$^{-/-}$*;tfec*$^{-/-}$;*mitfa*:GFP embryos than in the control (1) (****P*=0.0007). However, *mitfa*$^{-/-}$*;tfec*$^{-/-}$ mutants contain cNCCs posterior to the optic field (2). (C) Serial sections of *mitfa*$^{-/-}$*;tfec*$^{+/+}$;*mitfa*:GFP and *mitfa*$^{-/-}$*;tfec*$^{-/-}$;*mitfa*:GFP embryos at 48 hpf demonstrate that *mitfa*$^{-/-}$*;tfec*$^{-/-}$ mutants possess fewer cNCCs in the POM surrounding the eyes. Dorsal is upwards in the images in B,C. Data are mean±s.e.m. Scale bars: 100 μm in A; 50 μm in B,C.

composed of transplanted cells were used for subsequent analyses. Despite robust transplantation, wild-type retina/RPE cells failed to rescue colobomas in *mitfa*$^{-/-}$*;tfec*$^{-/-}$ mutants, even in cases in which they were largely restricted to the ventral optic cup (Fig. 3D, Fig. S4C). The maximum angle of CF opening in non-transplanted mutant eyes was 26.9°±3.04°, whereas in *mitfa*$^{-/-}$*;tfec*$^{-/-}$ mutants containing wild-type retina/RPE it was 39.82°±4.87° (*P*=0.037; Fig. 3E). Transplantation of wild-type cells into the retina/RPE of *mitfa*$^{-/-}$*;tfec*$^{+/+}$ embryos had no effect on CF closure (Fig. S4B). These data indicate that Mitf-family function in the retina/RPE probably does not facilitate CF closure. Two caveats here are that our transplants could be subthreshold for the number of cells necessary to mediate effective closure, or that transplanted wild-type cells could cease to behave/function as true wild types when located in a *mitfa*$^{-/-}$*;tfec*$^{-/-}$ optic cup. The fact that closure was not rescued in *mitfa*$^{-/-}$*;tfec*$^{-/-}$ embryos in which transplanted wild-type retina/RPE cells were largely restricted to the ventral optic cup suggests that the former is unlikely; however, the fact that some *mitfa*$^{-/-}$*;tfec*$^{-/-}$ mutants transplanted with wild-type retina/RPE cells actually had more severe colobomas than the non-transplanted *mitfa*$^{-/-}$*;tfec*$^{-/-}$ embryos, indicates that the latter caveat might be possible. It will be of interest to determine the molecular and cellular effects of Mitf and Tfec loss on both optic cup cells and cNCCs to determine the molecular underpinnings of these defects.

To further test the hypothesis that Mitf-family function in cNCCs is sufficient to mediate CF closure, we expressed wild-type *tfec* within cNCCs of *mitfa*$^{-/-}$*;tfec*$^{-/-}$ mutants and assessed CF closure. *tfec* is enriched at the CF during CF closure (Cao et al., 2018) and wild-type *tfec* is sufficient for CF closure in *mitfa*$^{-/-}$ mutants (Fig. 1, Fig. S1). Using the Tol2 system (Kwan et al., 2007), we generated pDestTol2pA2-*sox10*:mCherry-nostop-t2A-FLAG-*tfec*-pA and injected embryos derived from *mitfa*$^{-/-}$*;tfec*$^{+/-}$*;sox10:*eGFP incrosses. Embryos that possessed detectable mCherry^{+} cNCCs were assessed at 4 dpf for colobomas, sectioned serially and the maximum angle of CF opening quantified. Expression of wild-type *tfec* in *mitfa*$^{-/-}$*;tfec*$^{-/-}$ mutants reduced the CF opening from 20.58°±4.31° to 9.66°±2.49° (*P*=0.033; Fig. 3E). Control embryos retained no mCherry^{+} expression, which correlated with a lack of CF closure (Fig. 3F). Quantification of the number of *sox10*:eGFP^{+} cells revealed that expression of wild-type *tfec* in *mitfa*$^{-/-}$*;tfec*$^{-/-}$ mutants also rescued the localization of endogenous *sox10*:eGFP^{+} cNCCs within the cranial field (*P*=0.023; Fig. 3F). These data indicate that the localization of cNCCs can be rescued by the presence of wild-type *tfec*, and also that cNCCs outside of the *mitfa* lineage are affected by the loss of *mitfa* and *tfec*.

Development (2020) 147, dev187047. doi:10.1242/dev.187047

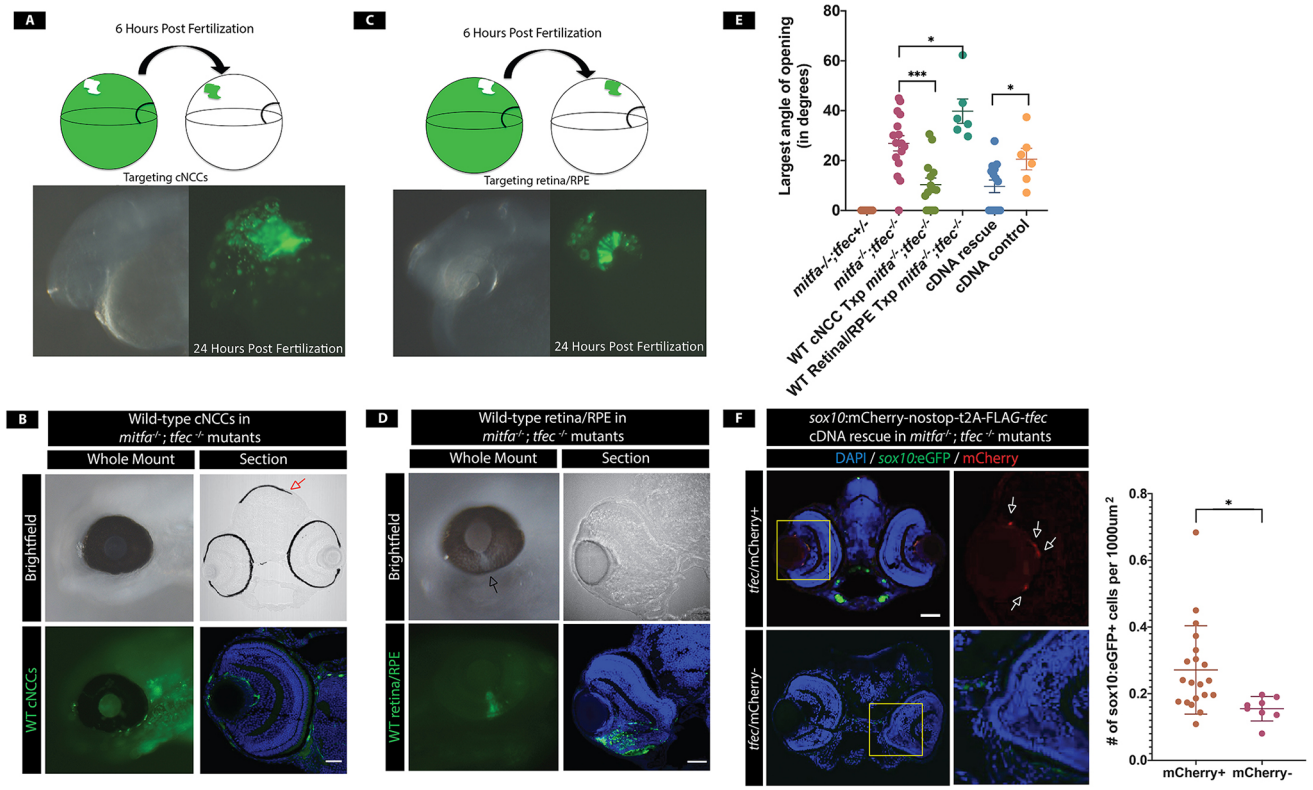

Fig. 3. *mitfa* and *tfec* are required within cNCCs to promote CF closure. (A) NCC transplantations. At 6 hpf, wild-type dextran-labeled cells are transplanted into the cNCC-fated region of a *mitfa*$^{-/-}$;*tfec*$^{-/-}$ embryo. At 24 hpf, transplanted cells are detected in the cNCC population. (B) Example of 4 dpf wild-type (WT) cNCC transplanted *mitfa*$^{-/-}$;*tfec*$^{-/-}$ embryo in which the coloboma has been rescued. Transplanted cNCCs are detected in and around the eye and rescue cNCC-derived pigmented melanocytes (red arrow) confirming successful transplantation. Scale bar: 25 µm. (C) Retina/RPE transplants. At 6 hpf, wild-type dextran-labeled cells are transplanted into the RPE/retinal-fated region of a *mitfa*$^{-/-}$;*tfec*$^{-/-}$ mutant. At 24 hpf, transplanted cells are detected within the eye, indicating successful transplantation. (D) At 4 dpf, transplanted embryos still possess colobomas. Arrow indicates a coloboma in the retina/RPE transplanted eye. (E) Quantification of colobomas (largest angle of CF opening) in rescue experiments. CF opening is significantly reduced in *mitfa*$^{-/-}$;*tfec*$^{-/-}$ embryos transplanted with wild-type cNCCs (P=0.0004, n=14 eyes). However, colobomas are not resolved in embryos transplanted with wild-type retina/RPE cells and are actually larger than in non-transplanted control *mitfa*$^{-/-}$;*tfec*$^{-/-}$ mutants (P=0.037, n=6 eyes). *tfec* cDNA injection also rescues colobomas (P=0.033, n=14 eyes). (F) pDestTol2pA2-*sox10*:mCherry-nostop-t2A-FLAG-*tfec*-pA injection reduces CF opening in *mitfa*$^{-/-}$;*tfec*$^{-/-}$ mutants. Arrows indicate mCherry^{+} (rescued) neural crest cells. Quantification of *sox10*:eGFP^{+} cells shows rescue of cNCCs within the eye field (P=0.023, n=20 mCherry^{+}, n=8 mCherry^{-} eyes). *P<0.05, ***P<0.001. Dorsal is upwards in all images. Data are mean±s.e.m. Scale bars: 25 µm (B,D); 50 µm (F).

In summary, these data identify defects in cNCC localization in *mitfa*$^{-/-}$;*tfec*$^{-/-}$ mutants and defects in BM breakdown in the CF, a function attributed to the POM (Gestri et al., 2018; James et al., 2016). Data from cell-transplantation and cDNA rescue experiments demonstrate that Mitf-function in cNCCs is sufficient to rescue CF closure in *mitfa*$^{-/-}$;*tfec*$^{-/-}$ mutants. Taken together, these data support a model in which Mitf-family function is required in cNCCs to facilitate CF closure. Without sufficient cNCC contribution/function within the POM, colobomas result. These data are consistent with those from other studies implicating cNCCs as crucial regulators of optic cup morphogenesis (Bryan et al., 2020; Fuhrmann et al., 2000). Additionally, they highlight the expanding role of Mitf-family TFs in a variety of developmental processes beyond their well-known roles in regulating pigmentation. Finally, these data identify a potential cellular mechanism underlying colobomas in COMMAD individuals with *MITF* mutations (George et al., 2016). Several human congenital disorders/syndromes that include colobomas also have phenotypes consistent with NCC defects (e.g. Akula et al., 2019; Asad et al., 2016). Further studies can now focus on the NCC origin of ocular diseases and how cNCCs modulate optic cup morphogenesis and CF closure. Future studies addressing these topics will be essential for understanding the link between NCC functions and congenital disorders of eye formation.

MATERIALS AND METHODS

Zebrafish husbandry

Zebrafish (*Danio rerio*) were maintained on a 14 h/10 h light-dark cycle at 28.5°C. For the *mitfa* and *tfec* lines, fish were maintained in a *mitfa*$^{-/-}$ mutant background and double mutant embryos were obtained by mating pairwise heterozygous *tfec*$^{+/-}$ crosses. The mutant alleles *mitfa*^{w2} (Lister et al., 1999) and *tfec*^{vc60} (Petratou et al., 2019 preprint) were used for all experiments. Wild-type AB animals were used as donors for rescue transplantation experiments. Fish genotyping was performed using high resolution melt analysis with the following primers for tfec: forward, GTGATATGCGCTGGAACAAAGGGA; reverse, GCTCTTTCTGCAGCCACTTAATGTAT. *sox10*:eGFP fish were generated previously (Hoffman et al., 2007) and obtained from Dr. Ann Morris (University of Kentucky, Lexington, USA). All fish were housed and maintained in accordance with the University of Pittsburgh School of Medicine Institutional Animal Care and Use Committee.

Tissue preparation and cryosectioning

Embryos were collected and fixed in 4% paraformaldehyde (PFA) in PBS for 1 h at room temperature. Embryos were subsequently washed with 25% and 35% sucrose in PBS, and embedded in Tissue Plus optimal cutting

Development (2020) 147, dev187047. doi:10.1242/dev.187047

temperature compound (Fisher Scientific). Tissue blocks were frozen and maintained at −80°C. Tissue sections (12 µm) were cut on polylysine-coated FrostPlus slides (Fisher Scientific). Slides were maintained at 4°C until analyzed.

Immunohistochemistry

Slides were rehydrated with three 20-min washes in 1× PBS. For laminin staining, antigen retrieval was performed by incubation in 0.5% SDS at 37°C for 20 min. Slides were washed in PBS and then blocked using 10% normal goat serum in PBS for 1 h. Staining was performed overnight at 4°C in blocking solution. The antibodies used in this study were as follows: anti-laminin1 (1:100; Sigma-Aldrich, L9393) 1:100 and goat anti-rabbit Alexa 488 secondary (1:500; Jackson ImmunoResearch, 111-545-144) 1:500. DNA was counterstained with DAPI (1:100; Life Technologies).

cNCC quantification and TUNEL assay at 24 hpf

*mitfa:*GFP embryos were collected at 24 hpf and fixed in 4% PFA in PBS for 1 h at room temperature. Genotyping and tissue preparation of embryos were performed as outlined above. Tissue was sectioned (12 µm) and an *In Situ* Cell Death Detection Kit, TMR red (Roche) was used to assess cell death. Cell death and quantification of total NCCs was ascertained by counting the total number of cranial *mitfa*:GFP cells and *mitfa*:GFP^{+} TUNEL^{+} cells in each half of the embryo. Numbers were normalized to the area of the eye in the respective side of the head and results were displayed as the number of NCCs/per 1000 µm^{2} area of the eye.

Imaging

Slides were imaged using an Olympus FV1200 confocal microscope and Olympus software. Ten to 12 1 µm optical sections were acquired and then stacked using ImageJ software (https://imagej.nih.gov/ij/).

Whole-mount imaging was performed using an Olympus FV1200 confocal microscope. Embryos were mounted in 0.5% low melt agarose and then immersed in Danieu's embryo media. Embryos were imaged *in vivo* for 15 h starting at 25 hpf and analyzed using Olympus software.

Transplantation assays

Fish lines were bred as outlined above. Donor embryos were injected with 3.5% Alexa Fluor Dextran 488 (Thermo Fisher Scientific, D22910). Embryos were maintained in Danieu's embryo media and dechorionated at 4 hpf. At 6 hpf, embryos were embedded in 1.5% methylcellulose and two drops of Ringer's high calcium solution. For transplant rescue experiments, 10-15 dextran^{+} cells of a wild-type embryo were transferred into the region of neural crest or retinal/RPE origin in a *mitfa*$^{-/-}$;*tfec*$^{-/-}$ embryo. Embryos were then maintained in sterile filtered Danieu's embryo media with 1× pen/strep for 24 h. At 24 h, embryos were assessed for successful transplantation using a Zeiss Axio Zoom V16 Dissecting Microscope and Z3 Zeiss software. For retinal/RPE transplants, we required that at least 20% of the optic cup (primarily ventral optic cup) was composed of dextran^{+} cells to be considered a successful transplant. Embryos were grown until 4 dpf, at which point they were assessed for the presence or absence of colobomas. Transplanted embryos were assessed from three independent experiments. The preparation of tissue included collection, fixation, transverse sectioning and imaging as described previously. Images were analyzed to determine the presence and quantification of the angle of the CF opening.

Quantification of CF opening

To quantify the CF opening, ImageJ was used to define a line between the dorsal and ventral inner plexiform boundaries of the retina. From the central point on this line, the angle of opening of the CF was calculated from each section. Mild mutants were defined as possessing CF openings smaller than 20°; moderate openings were defined as 20°-35°; and severe openings were larger than 35°.

cDNA injections

The plasmid pDestTol2pA2-*sox10*:mCherry-nostop-t2A-FLAG-*tfec*-pA used for cDNA microinjection was generated by multisite Gateway cloning (Invitrogen/Thermo Fisher Scientific) from the plasmids pDestTol2pA2 (Kwan et al., 2007; Tol2Kit, 394), p5E-MCS-sox10-4.8 (Prendergast et al., 2012), pME-mCherry-no stop (Kwan et al., 2007; Tol2Kit, 456) and p3E-2A-FLAG-tfec-pA (Petratou et al. 2019). Control cDNA embryos were microinjected but retained no mCherry^{+} cells within the cranial region, therefore the construct was not successfully incorporated.

Statistics

Student's *t*-test (unpaired and two tailed) was used to assess significance and data are mean±s.e.m.

Acknowledgements

We thank Kira Lathrop and the University of Pittsburgh Ophthalmology Imaging Core for advice on imaging; Hugh Hammer of the University of Pittsburgh Fish Facility for help and guidance on fish maintenance; and Corin Tucker, Carrie Brownstein and Janet Weiss for technical support.

Competing interests

The authors declare no competing or financial interests.

Author contributions

Conceptualization: K.L.S., J.A.L., J.M.G.; Formal analysis: K.L.S.; Investigation: K.L.S., A.M.L.-P., S.M.G.; Resources: S.A.S., J.A.L.; Writing - original draft: K.L.S.; Writing - review & editing: K.L.S., J.A.L., J.M.G.; Visualization: K.L.S.; Supervision: J.M.G.; Project administration: J.M.G.; Funding acquisition: J.M.G.

Funding

This work was supported by the National Institutes of Health (NIH) (NIH R01-EY18005 to J.M.G., T32-EY17271 to K.L.S. and UL1TR00058 to J.A.L.) and by the AD Williams' Fund of Virginia Commonwealth University (S.A.S. and J.A.L.). We also acknowledge support from the National Institutes of Health Core Grant P30 EY08098 to the Department of Ophthalmology, from the Eye and Ear Foundation of Pittsburgh, and from an unrestricted grant from Research to Prevent Blindness. Deposited in PMC for release after 12 months.

Supplementary information

Supplementary information available online at
https://dev.biologists.org/lookup/doi/10.1242/dev.187047.supplemental

Peer review history

The peer review history is available online at
https://dev.biologists.org/lookup/doi/10.1242/dev.187047.reviewer-comments.pdf

References

Akula, M., Park, J. W. and West-Mays, J. A. (2019). Relationship between neural crest cell specification and rare ocular diseases. *J. Neurosci. Res.* **97**, 7-15. doi:10.1002/jnr.24245

ALSomiry, A. S., Gregory-Evans, C. Y. and Gregory-Evans, K. (2019). An update on the genetics of ocular coloboma. *Hum. Genet.* **138**, 865-880. doi:10.1007/s00439-019-02019-3

Asad, Z., Pandey, A., Babu, A., Sun, Y., Shevade, K., Kapoor, S., Ullah, I., Ranjan, S., Scaria, V., Bajpai, R., et al. (2016). Rescue of neural crest-derived phenotypes in a zebrafish CHARGE model by Sox10 downregulation. *Hum. Mol. Genet.* **25**, 3539-3554. doi:10.1093/hmg/ddw198

Barbieri, A. M., Broccoli, V., Bovolenta, P., Alfano, G., Marchitiello, A., Mocchetti, C., Crippa, L., Bulfone, A., Marigo, V., Ballabio, A., et al. (2002). Vax2 inactivation in mouse determines alteration of the eye dorsal-ventral axis, misrouting of the optic fibres and eye coloboma. *Development* **129**, 805-813.

Bermejo, E. and Martínez-Frías, M. L. (1998). Congenital eye malformations: clinical-epidemiological analysis of 1,124,654 consecutive births in Spain. *Am. J. Med. Genet.* **75**, 497-504. <497::AID-AJMG8>3.0.CO;2-K

Bernstein, C. S., Anderson, M. T., Gohel, C., Slater, K., Gross, J. M. and Agarwala, S. (2018). The cellular bases of choroid fissure formation and closure. *Dev. Biol.* **440**, 137-151. doi:10.1016/j.ydbio.2018.05.010

Bharti, K., Liu, W., Csermely, T., Bertuzzi, S. and Arnheiter, H. (2008). Alternative promoter use in eye development: the complex role and regulation of the transcription factor MITF. *Development* **135**, 1169-1178. doi:10.1242/dev.014142

Bharti, K., Gasper, M., Ou, J., Brucato, M., Clore-Gronenborn, K., Pickel, J. and Arnheiter, H. (2012). A regulatory loop involving PAX6, MITF, and WNT signaling controls retinal pigment epithelium development. *PLoS Genet.* **8**, e1002757. doi:10.1371/journal.pgen.1002757

Bibliowicz, J., Tittle, R. K. and Gross, J. M. (2011). Toward a better understanding of human eye disease: Insights from the zebrafish, Danio rerio. *Prog. Mol. Biol. Transl. Sci.* **100**, 287-330. doi:10.1016/B978-0-12-384878-9.00007-8

Bohnsack, B. L., Gallina, D., Thompson, H., Kasprick, D. S., Lucarelli, M. J., Dootz, G., Nelson, C., McGonnell, I. M. and Kahana, A. (2011). Development of

extraocular muscles requires early signals from periocular neural crest and the developing eye. *Arch. Ophthalmol. (Chicago, Ill. 1960)* **129**, 1030-1041. doi:10.1001/archophthalmol.2011.75

Bryan, C. D., Casey, M. A., Pfeiffer, R. L., Jones, B. W. and Kwan, K. M. (2020). Optic cup morphogenesis requires neural crest-mediated basement membrane assembly. *Development* **147**, dev181420. doi:10.1242/dev.181420

Cao, M., Ouyang, J., Liang, H., Guo, J., Lin, S., Yang, S., Xie, T. and Chen, S. (2018). Regional gene expression profile comparison reveals the unique transcriptome of the optic fissure. *Investig. Opthalmology Vis. Sci.* **59**, 5773. doi:10.1167/iovs.18-23962

Capowski, E. E., Simonett, J. M., Clark, E. M., Wright, L. S., Howden, S. E., Wallace, K. A., Petelinsek, A. M., Pinilla, I., Phillips, M. J., Meyer, J. S., et al. (2014). Loss of MITF expression during human embryonic stem cell differentiation disrupts retinal pigment epithelium development and optic vesicle cell proliferation. *Hum. Mol. Genet.* **23**, 6332-6344. doi:10.1093/hmg/ddu351

Carmany-Rampey, A. and Moens, C. B. (2006) Modern mosaic analysis in the zebrafish. *Methods (San Diego, Calif.)*. **39**, 228-238. doi:10.1016/j.ymeth.2006.02.002

Carrara, N., Weaver, M., Piedade, W. P., Vöcking, O. and Famulski, J. K. (2019). Temporal characterization of optic fissure basement membrane composition suggests nidogen may be an initial target of remodeling. *Dev. Biol.* **452**, 43-54. doi:10.1016/j.ydbio.2019.04.012

Cavodeassi, F. and Bovolenta, P. (2014). New functions for old genes: Pax6 and Mitf in eye pigment biogenesis. *Pigment Cell Melanoma Res.* **27**, 1005-1007. doi:10.1111/pcmr.12308

Chang, L., Blain, D., Bertuzzi, S. and Brooks, B. P. (2006). Uveal coloboma: clinical and basic science update. *Curr. Opin. Ophthalmol.* **17**, 447-470. doi:10.1097/01.icu.0000243020.82380.f6

Christiansen, J. H., Coles, E. G. and Wilkinson, D. G. (2000). Molecular control of neural crest formation, migration and differentiation. *Curr. Opin. Cell Biol.* **12**, 719-724. doi:10.1016/S0955-0674(00)00158-7

Curran, K., Raible, D. W. and Lister, J. A. (2009). Foxd3 controls melanophore specification in the zebrafish neural crest by regulation of Mitf. *Dev. Biol.* **332**, 408-417. doi:10.1016/j.ydbio.2009.06.010

Dee, C. T., Szymoniuk, C. R., Mills, P. E. D. and Takahashi, T. (2013). Defective neural crest migration revealed by a Zebrafish model of Alx1-related frontonasal dysplasia. *Hum. Mol. Genet.* **22**, 239-251. doi:10.1093/hmg/dds423

FitzPatrick, D. R. (2005). Developmental eye disorders. *Curr. Opin. Genet. Dev.* **15**, 348-353. doi:10.1016/j.gde.2005.04.013

Fuhrmann, S. (2010). Eye morphogenesis and patterning of the optic vesicle. *Curr. Top. Dev. Biol.* **93**, 61-84. doi:10.1016/B978-0-12-385044-7.00003-5

Fuhrmann, S., Levine, E. M. and Reh, T. A. (2000). Extraocular mesenchyme patterns the optic vesicle during early eye development in the embryonic chick. *Development* **127**, 4599-4609.

Geeraets, R. (1976). An electron microscopic study of the closure of the optic fissure in the golden hamster. *Am. J. Anat.* **145**, 411-431. doi:10.1002/aja.1001450402

George, A., Zand, D. J., Hufnagel, R. B., Sharma, R., Sergeev, Y. V., Legare, J. M., Rice, G. M., Scott Schwoerer, J. A., Rius, M., Tetri, L., et al. (2016). Biallelic mutations in MITF cause coloboma, osteopetrosis, microphthalmia, macrocephaly, albinism, and deafness. *Am. J. Hum. Genet.* **99**, 1388-1394. doi:10.1016/j.ajhg.2016.11.004

Gestri, G., Bazin-Lopez, N., Scholes, C. and Wilson, S. W. (2018). Cell behaviors during closure of the choroid fissure in the developing eye. *Front. Cell. Neurosci.* **12**. doi:10.3389/fncel.2018.00042

Gregory-Evans, C. Y., Williams, M. J., Halford, S. and Gregory-Evans, K. (2004). Ocular coloboma: a reassessment in the age of molecular neuroscience. *J. Med. Genet.* **41**, 881-891. doi:10.1136/jmg.2004.025494

Grocott, T., Johnson, S., Bailey, A. P. and Streit, A. (2011). Neural crest cells organize the eye via TGF-β and canonical Wnt signalling. *Nat. Commun.* **2**, 265. doi:10.1038/ncomms1269

Hemesath, T. J., Steingrímsson, E., McGill, G., Hansen, M. J., Vaught, J., Hodgkinson, C. A., Arnheiter, H., Copeland, N. G., Jenkins, N. A. and Fisher, D. E. (1994). Microphthalmia, a critical factor in melanocyte development, defines a discrete transcription factor family. *Genes Dev.* **8**, 2770-2780. doi:10.1101/gad.8.22.2770

Hero, I. (1989). The optic fissure in the normal and microphthalmic mouse. *Exp. Eye Res.* **49**, 229-239. doi:10.1016/0014-4835(89)90093-6

Hero, I. (1990). Optic fissure closure in the normal cinnamon mouse: An ultrastructural study. *Investig. Ophthalmol. Vis. Sci.* **31**, 197-216.

Hero, I., Farjah, M. and Scholtz, C. L. (1991). The prenatal development of the optic fissure in colobomatous microphthalmia. *Investig. Ophthalmol. Vis. Sci.* **32**, 2622-2635.

Hodgkinson, C. A., Moore, K. J., Nakayama, A., Steingrímsson, E., Copeland, N. G., Jenkins, N. A. and Arnheiter, H. (1993). Mutations at the mouse microphthalmia locus are associated with defects in a gene encoding a novel basic-helix-loop-helix-zipper protein. *Cell* **74**, 395-404. doi:10.1016/0092-8674(93)90429-T

Hoffman, T. L., Javier, A. L., Campeau, S. A., Knight, R. D. and Schilling, T. F. (2007). Tfap2 transcription factors in zebrafish neural crest development and ectodermal evolution. *J. Exp. Zool. Part B Mol. Dev. Evol.* **308B**, 679-691. doi:10.1002/jez.b.21189

Hsiao, J. J. and Fisher, D. E. (2014). The roles of microphthalmia-associated transcription factor and pigmentation in melanoma. *Arch. Biochem. Biophys* **563**, 28-34. doi:10.1016/j.abb.2014.07.019

James, A., Lee, C., Williams, A. M., Angileri, K., Lathrop, K. L. and Gross, J. M. (2016). The hyaloid vasculature facilitates basement membrane breakdown during choroid fissure closure in the zebrafish eye. *Dev. Biol.* **419**, 262-272. doi:10.1016/j.ydbio.2016.09.008

Jeffery, G. (1998). The retinal pigment epithelium as a developmental regulator of the neural retina. *Eye* (Lond) **12**, 499-503. doi:10.1038/eye.1998.137

Kaucka, M., Ivashkin, E., Gyllborg, D., Zikmund, T., Tesarova, M., Kaiser, J., Xie, M., Petersen, J., Pachnis, V., Nicolis, S. K., et al. (2016). Analysis of neural crest-derived clones reveals novel aspects of facial development. *Sci. Adv.* **2**, e1600060. doi:10.1126/sciadv.1600060

Kawakami, A. and Fisher, D. E. (2017). The master role of microphthalmia-associated transcription factor in melanocyte and melanoma biology. *Lab. Invest.* **97**, 649-656. doi:10.1038/labinvest.2017.9

Kwan, K. M., Fujimoto, E., Grabher, C., Mangum, B. D., Hardy, M. E., Campbell, D. S., Parant, J. M., Yost, H. J., Kanki, J. P. and Chien, C.-B. (2007). The Tol2kit: A multisite gateway-based construction kit forTol2 transposon transgenesis constructs. *Dev. Dyn* **236**, 3088-3099. doi:10.1002/dvdy.21343

Langenberg, T., Kahana, A., Wszalek, J. A. and Halloran, M. C. (2008). The eye organizes neural crest cell migration. *Dev. Dyn* **237**, 1645-1652. doi:10.1002/dvdy.21577

Lee, J. and Gross, J. M. (2007). Laminin β1 and γ1 containing laminins are essential for basement membrane integrity in the zebrafish eye. *Invest. Ophthalmol. Vis. Sci.* **48**, 2483-2490. doi:10.1167/iovs.06-1211

Lister, J. A. (1999). Zebrafish Mitf-related gene nacre. *Development* **126**, 3757-3767.

Lister, J. A., Robertson, C. P., Lepage, T., Johnson, S. L. and Raible, D. W. (1999). Nacre encodes a zebrafish microphthalmia-related protein that regulates neural-crest-derived pigment cell fate. *Development* **126**, 3757-3767.

Lister, J. A., Close, J. and Raible, D. W. (2001). Duplicate mitf genes in Zebrafish: complementary expression and conservation of melanogenic potential. *Dev. Biol.* **237**, 333-344. doi:10.1006/dbio.2001.0379

Lister, J. A., Lane, B. M., Nguyen, A. and Lunney, K. (2011). Embryonic expression of zebrafish MiT family genes Tfe3b, Tfeb, and Tfec. *Dev. Dyn.* **240**, 2529-2538. doi:10.1002/dvdy.22743

Lupo, G., Gestri, G., O'Brien, M., Denton, R. M., Chandraratna, R. A. S., Ley, S. V., Harris, W. A. and Wilson, S. W. (2011). Retinoic acid receptor signaling regulates choroid fissure closure through independent mechanisms in the ventral optic cup and periocular mesenchyme. *Proc. Natl. Acad. Sci. USA* **108**, 8698-8703. doi:10.1073/pnas.1103802108

Ma, X., Li, H., Chen, Y., Yang, J., Chen, H., Arnheiter, H., and Hou, L. (2019) The transcription factor MITF in RPE function and dysfunction. *Prog. Retin. Eye Res.* **73**, 100766. doi:10.1016/j.preteyeres.2019.06.002

Martina, J. A., Diab, H. I., Li, H. and Puertollano, R. (2014). Novel roles for the MiTF/TFE family of transcription factors in organelle biogenesis, nutrient sensing, and energy homeostasis. *Cell. Mol. Life Sci.* **71**, 2483-2497. doi:10.1007/s00018-014-1565-8

McMahon, C., Gestri, G., Wilson, S. W. and Link, B. A. (2009). Lmx1b is essential for survival of periocular mesenchymal cells and influences Fgf-mediated retinal patterning in zebrafish. *Dev. Biol.* **332**, 287-298. doi:10.1016/j.ydbio.2009.05.577

Onwochei, B. C., Simon, J. W., Bateman, J. B., Couture, K. C. and Mir, E. (2000). Ocular colobomata. *Surv. Ophthalmol.* **45**, 175-194. doi:10.1016/S0039-6257(00)00151-X

Petratou, K., Spencer, S. A., Kelsh, R. N. and Lister, J. A. (2019). The MITF paralog tfec is required in neural crest development for fate specification of the iridophore lineage from a multipotent pigment cell progenitor. *bioRxiv*, 862011. doi:10.1101/862011

Pogenberg, V., Ogmundsdóttir, M. H., Bergsteinsdóttir, K., Schepsky, A., Phung, B., Deineko, V., Milewski, M., Steingrímsson, E. and Wilmanns, M. (2012). Restricted leucine zipper dimerization and specificity of DNA recognition of the melanocyte master regulator MITF. *Genes Dev.* **26**, 2647-2658. doi:10.1101/gad.198192.112

Prendergast, A., Linbo, T. H., Swarts, T., Ungos, J. M., McGraw, H. F., Krispin, S., Weinstein, B. M. and Raible, D. W. (2012). The metalloproteinase inhibitor Reck is essential for zebrafish DRG development. *Development* **139**, 1141-1152. doi:10.1242/dev.072439

Price, E. R. and Fisher, D. E. (2001). Sensorineural deafness and pigmentation genes: melanocytes and the Mitf transcriptional network. *Neuron* **30**, 15-18. doi:10.1016/S0896-6273(01)00259-8

Reissmann, M. and Ludwig, A. (2013). Pleiotropic effects of coat colour-associated mutations in humans, mice and other mammals. *Semin. Cell Dev. Biol.* **24**, 576-586. doi:10.1016/j.semcdb.2013.03.14

Schimmenti, L. A., de la Cruz, J., Lewis, R. A., Karkera, J. D., Manligas, G. S., Roessler, E. and Muenke, M. (2003). Novel mutation in sonic hedgehog in non-

syndromic colobomatous microphthalmia. *Am. J. Med. Genet.* **116A**, 215-221. doi:10.1002/ajmg.a.10884

Schmitt, E. A. and Dowling, J. E. (1994). Early-eye morphogenesis in the zebrafish, Brachydanio rerio. *J. Comp. Neurol.* **344**, 532-542. doi:10.1002/cne.903440404

Sedykh, I., Yoon, B., Roberson, L., Moskvin, O., Dewey, C. N. and Grinblat, Y. (2017). Zebrafish zic2 controls formation of periocular neural crest and choroid fissure morphogenesis. *Dev. Biol.* **429**, 92-104. doi:10.1016/j.ydbio.2017.07.003

See, A. W.-M. and Clagett-Dame, M. (2009). The temporal requirement for vitamin A in the developing eye: mechanism of action in optic fissure closure and new roles for the vitamin in regulating cell proliferation and adhesion in the embryonic retina. *Dev. Biol.* **325**, 94-105. doi:10.1016/j.ydbio.2008.09.030

Steingrímsson, E., Moore, K. J., Lamoreux, M. L., Ferré-D'amaré, A. R., Burley, S. K., Zimring, D. C. S., Skow, L. C., Hodgkinson, C. A., Arnheiter, H., Copeland, N. G., et al. (1994). Molecular basis of mouse microphthalmia (mi) mutations helps explain their developmental and phenotypic consequences. *Nat. Genet.* **8**, 256-263. doi:10.1038/ng1194-256

Steingrímsson, E., Copeland, N. G. and Jenkins, N. A. (2004). Melanocytes and the *Microphthalmia* transcription factor network. *Annu. Rev. Genet.* **38**, 365-411. doi:10.1146/annurev.genet.38.072902.092717

Stoll, C., Alembik, Y., Dott, B. and Roth, M. P. (1997). Congenital eye malformations in 212,479 consecutive births. *Ann. Genet.* **40**, 122-128.

Takebayashi, K., Chida, K., Tsukamoto, I., Morii, E., Munakata, H., Arnheiter, H., Kuroki, T., Kitamura, Y. and Nomura, S. (1996). The recessive phenotype displayed by a dominant negative microphthalmia-associated transcription factor mutant is a result of impaired nucleation potential. *Mol. Cell. Biol.* **16**, 1203-1211. doi:10.1128/MCB.16.3.1203

Tsuji, N., Kita, K., Ozaki, K., Narama, I. and Matsuura, T. (2012). Organogenesis of mild ocular coloboma in FLS mice: failure of basement membrane disintegration at optic fissure margins. *Exp. Eye Res.* **94**, 174-178. doi:10.1016/j.exer.2011.12.004

Williams, A. L. and Bohnsack, B. L. (2015). Neural crest derivatives in ocular development: Discerning the eye of the storm. *Birth Defects Res. Part C Embryo Today Rev.* **105**, 87-95. doi:10.1002/bdrc.21095

Woo, K. and Fraser, S. E. (1995). Order and coherence in the fate map of the zebrafish nervous system. *Development* **121**, 2595-2609.

Zhao, G. Q., Zhao, Q., Zhou, X., Mattei, M. G. and de Crombrugghe, B. (1993). TFEC, a basic helix-loop-helix protein, forms heterodimers with TFE3 and inhibits TFE3-dependent transcription activation. *Mol. Cell. Biol.* **13**, 4505-4512. doi:10.1128/MCB.13.8.4505

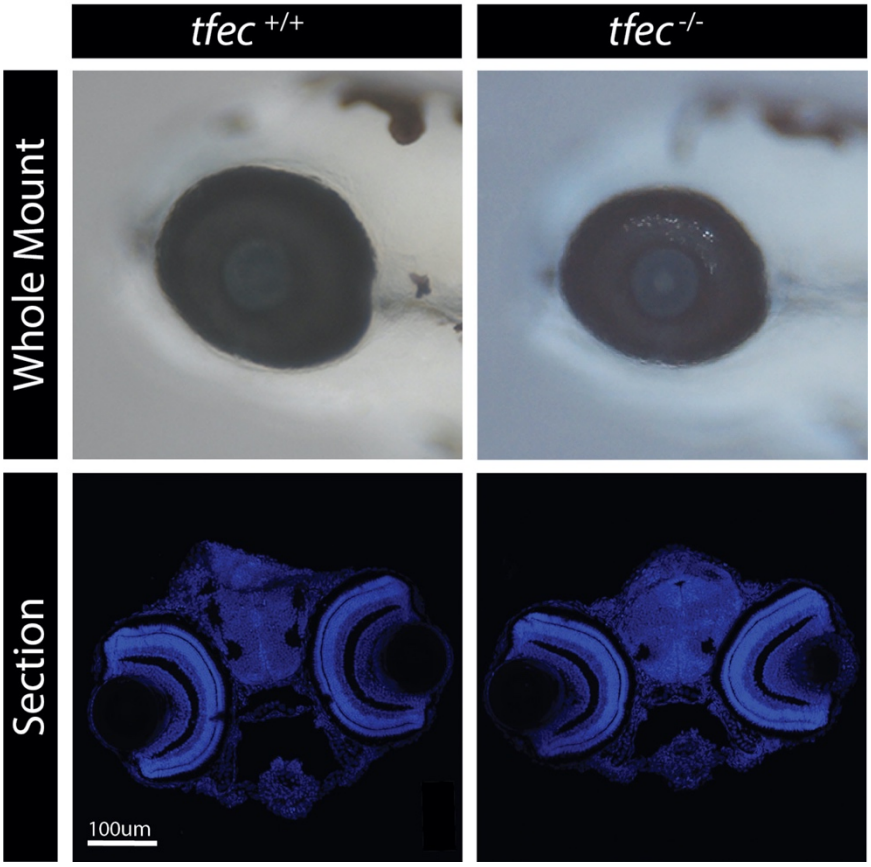

Figure S1. *tfec*$^{-/-}$ single mutants do not possess colobomas. Whole mount and transverse sections of 4dpf *tfec* $^{-/-}$ mutants reveals mild microphthalmia and pigmentation defects. No colobomas are detected. Dorsal is up in all images. Scale bar = 100μm.

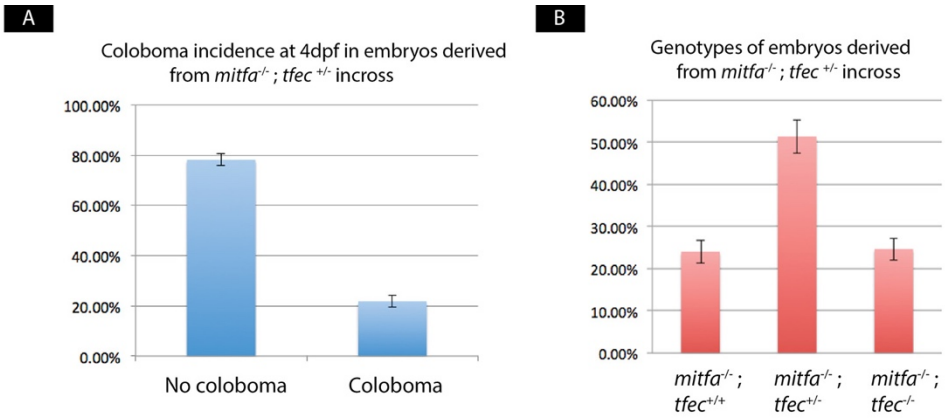

Figure S2. Quantification of colobomas in *mitfa* $^{-/-}$;*tfec* $^{+/-}$ incrosses. A) Coloboma incidence in embryos at 4dpf from *mitfa* $^{-/-}$;*tfec* $^{+/-}$ incrosses. On average 21% of embryos possessed colobomas of varying severity. (n=4 rounds of breeding) **B)** Genotypes of embryos in *mitfa* $^{-/-}$;*tfec* $^{+/-}$ incrosses. Expected Mendelian ratios of *mitfa* $^{-/-}$;*tfec* $^{+/+}$, *mitfa* $^{-/-}$; *tfec* $^{+/-}$, and *mitfa* $^{-/-}$;*tfec* $^{-/-}$ are observed (n= 4 rounds of breeding).

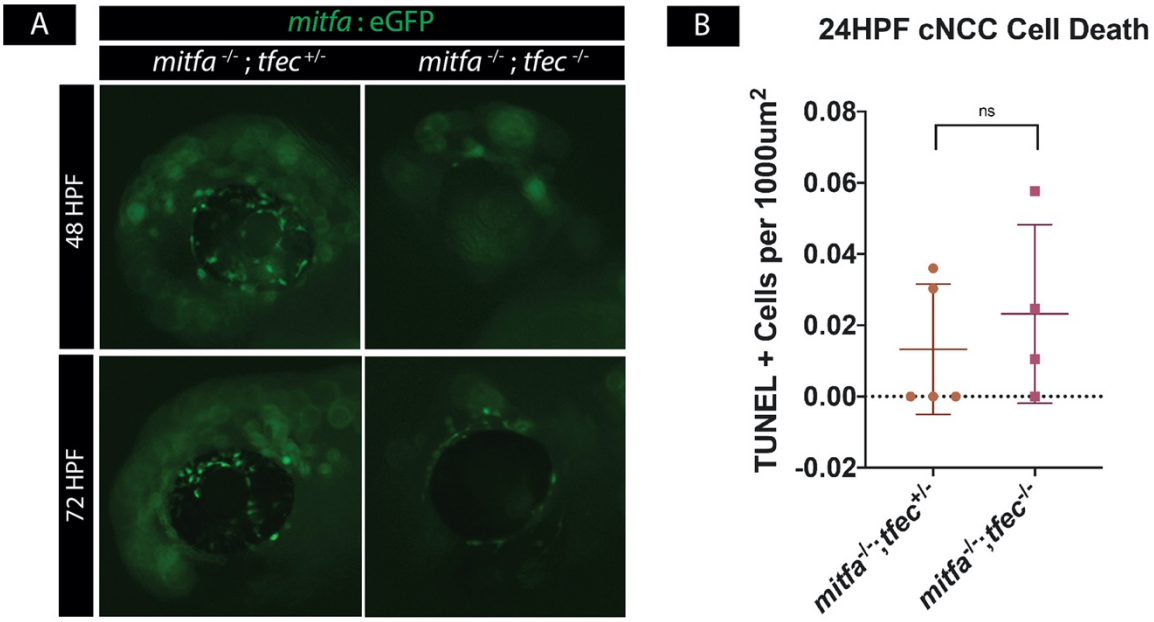

Figure S3. Loss of cNCCs in the POM is not the result cell death. A) Whole-mount images of *mitfa* $^{-/-}$*;tfec* $^{+/-}$ and *mitfa* $^{-/-}$*;tfec* $^{-/-}$ embryos reveals persistent loss of cNCC within the POM at 48hpf and 72hpf. **B)** Quantification of TUNEL^{+} cNCCs. While a trend of increased cell death is present, loss of cNCC numbers cannot be attributed solely to apoptosis at 24hpf (p=0.512, n=5 embryos).

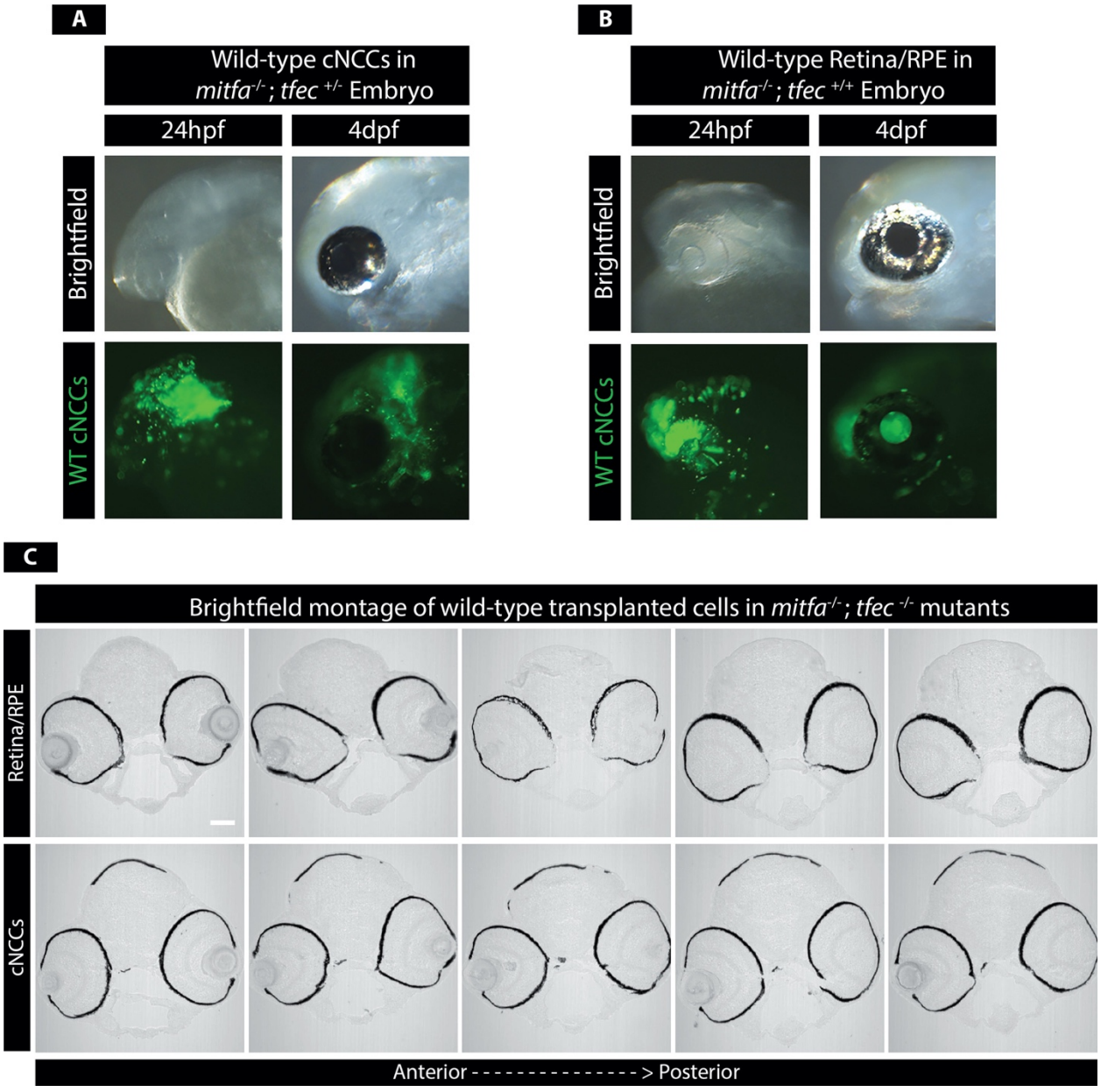

Figure S4. Transplantation of wild-type cells does not affect eye development. A) Wild-type cells transplanted into the region of cNCC origin in a *mitfa* $^{-/-}$*;tfec* $^{+/-}$ embryo shows no effect on eye development. **B)** Similarly, transplanted wild-types cells targeting the retina/RPE in *mitfa* $^{-/-}$*;tfec* $^{+/+}$ embryos show no effect on eye development. **C)** Serial sections of representative retina/RPE and cNCC transplanted embryos. CF closure phenotypes are only detected in retina/RPE cell transplanted embryos. Dorsal is up in all images. Scale bar = 100μm.

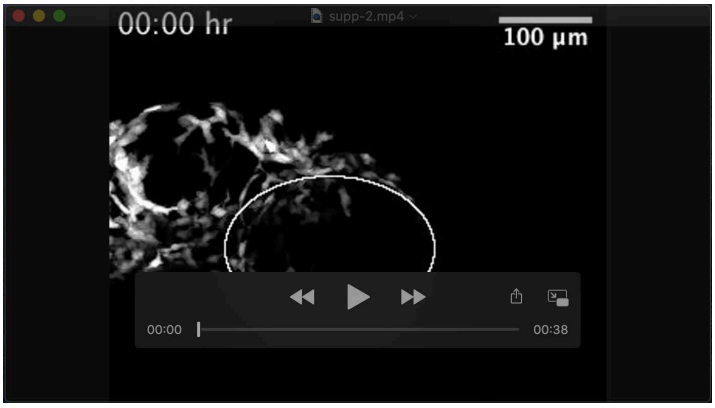

Movie 1: Wild-type embryos show normal migration of cNCCs starting at 25hpf. cNCCs can be seen migrating in and around the developing optic cup, eventually making their way around the entirety of the eye and into the choroid fissure.

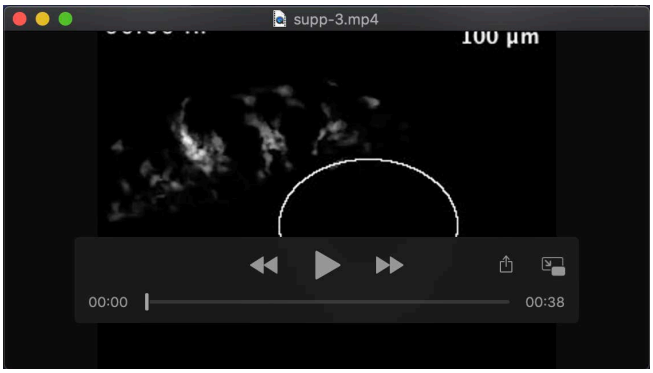

Movie 2: Mutant embryos show remarkably fewer neural crest cells at 25hpf. Already, there is a lack of migration of the cells into and around the eye. These cNCCs never reach the CF during the 15-hour time-lapse movie and instead stay in the dorsal portion of the developing head. cNCCs seem to lack direction and at t=8:08-10:08, several dorsal cNCCs burst, implicating increased cNCC cell death in *mitfa* $^{-/-}$*;tfec* $^{-/-}$ embryos.